A novel RF resonator using microstrip transmission line for human body MRI at 3T

Hyeok-Woo Son[1], Young-Ki Cho[1], Hyungsuk Yoo[2]
[1]School of Electronics Engineering, Kyungpook National University
80 Daehakro, Buk-gu, Daegu, 702-701, Korea
[2]Department of Biomedical Engineering, University of Ulsan
Department of Biomedical Engineering, University of Ulsan, Nam-gu, Ulsan, 680-749, Korea

***Abstract*- A square-slots loaded (SSL) radio frequency (RF) resonator using microstrip transmission line (MTL) is designed for a human body 3T MRI. The SSL RF resonator shows greater penetrated RF magnetic fields near the center of the phantom than traditional RF resonators using MTL. A multichannel coil using SSL RF resonators was also simulated and provides good parallel excitation performance. In addition, RF shimming for homogenization can be effectively controlled by adjusting the inputs of eight resonators. Numerical results were obtained using a spherical phantom and a realistic human body model at 3T to calculate B_1^+ fields.**

I. INTRODUCTION

High magnetic resonance imaging (MRI) systems (> 3 T) have good intrinsic SNR (signal-to-noise ratio), high resolution, and are used important instrument for clinical diagnosis of the human body [1]-[3]. One of the main challenges for these systems is B_1^+ inhomogeneity. To alleviate this problem, multi-channel radio frequency (RF) coils with parallel excitations are used [4,5]. They can provide higher B_1^+ fields in the region of interest (ROI) and can optimize the B_1^+ fields by driving the currents of individual coil elements. In this paper, these multichannel RF coils are applied to 3 T MRI systems, and a new RF resonator is proposed to enhance the multichannel coil performance. A general microstrip transmission line (MTL) resonator and a proposed square-slot loaded (SSL) resonator are simulated with a head phantom, to obtain the B_1^+ distribution. Then, an eight channel body coil with MTL resonators is replaced by the proposed SSL resonators for human body simulations. To determine the excitation parameters of the RF multichannel coils, convex optimization is used, and the SSL multichannel coil provides better B_1^+ fields. To the best of our knowledge, there are no previous analyses of multichannel RF coils in 3 T MRI systems. SSL resonators based on multichannel RF body coils can be used at hospitals for higher quality images.

II. METHOD

A. The MTL RF resonator

Figure 1 shows a RF resonator based on the use of microstrip transmission line(MTL). Low loss dielectric material Teflon (ε_r =2.08, loss tangent=0.004) was used as a substrate of microstrip with height (h) and length (l) of 2.0 cm and 15 cm, respectively, and microstrip line width (w) is 18 mm. The microstrip line is used as λ/2 resonator with its ends terminated capacitors. The terminated shunt capacitors are used to reduce the physical length and to match the desired Larmor frequency(123.5 MHz, 3T).

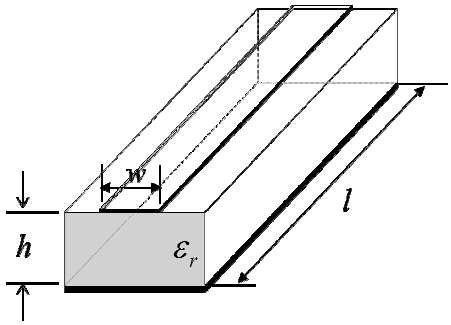

Figure 1. Illustration of microstrip transmission line (MTL)

B. The SLL RF resonator

The SSL RF resonator has a same dielectric material and size such as a general RF resonator in Fig. 2. The width and length of a square slot is 6 mm and 18 mm, respectively. The distance between adjacent square-slots and between square-slots along a longitudinal direction is 2 mm and 6 mm, respectively.

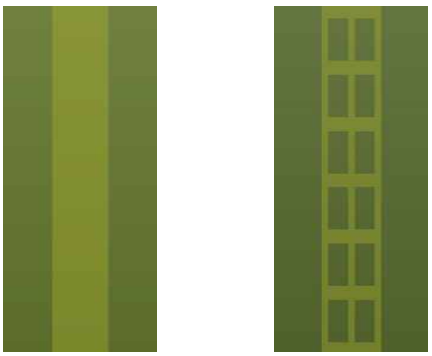

(a) (b)

Figure 2. RF resonators based on the use of microstrip transmission line. (a) a general RF resonator (b) squares-slot loaded(SSL) RF resonator

In this paper, the purpose of RF resonator design is to increase the penetrated magnetic field into an object. To increase penetrated magnetic field, the surface current density on strip conductor is also increased. The impact of loading squares-slot on strip conductor can be seen surface current density profiles in Fig. 3. In the general RF resonator,

the surface current density is concentrated at the edges of strip conductor. The surface current density of the SSL RF resonator is not only concentrated at the edges of strip conductor, but also in the center of strip conductor. As a result, penetrated magnetic field of a SSL RF resonator is anticipated more greater than a general RF resonator. Fig. 4 shows the penetrated RF magnetic field of a general RF resonator and a SSL RF resonator in a spherical phantom (ε_r=58.1, σ=0.539). The penetrated magnetic field of the SSL RF resonator is stronger than the general RF resonator at the center of the phantom.

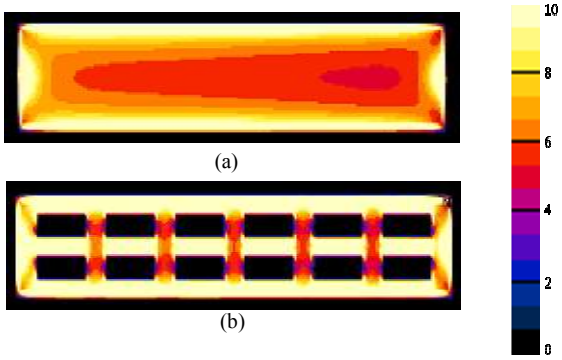

Figure 3. Surface current density (10^4 A/m^2) distribution of a general RF resonator (a) and a SSL RF resonator (b).

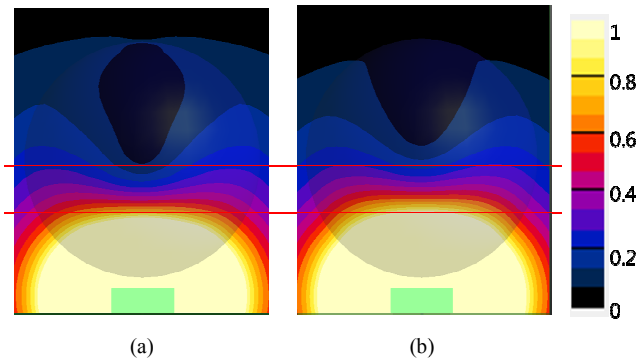

Figure 4. The penetrated magnetic field in the phantom of a general RF resonator (a) and a SSL RF resonator (b).

III. SIMULATION AND RESULTS

SEMCAD based on finite difference time-domain method was used to obtain B_1^+ and E field with human model [6]. Duke model from Virtual Family Models is used to simulate a realistic body model. A photograph of 8-channle body coil using SSL RF resonators with human model and a realistic body model including many different tissue types (e.g., heart, liver, lung, kidney, intervertebral disc, bone, fat, and so on) is shown Fig. 5. Before obtaining B_1^+ and E of 8-channel volume coil, the RF resonators with a spherical phantom (ε_r=58.1, σ=0.539 Siemens/m) were tuned to desired Larmor frequency by terminated shunt capacitors. When RF resonators are tuned, these capacitors are different capacitance between the a general RF resonator and the SSL RF resonator. The frequency response (S11) of RF resonators is shown in Fig. 6. The SSL RF resonator is better than the general RF resonator. It means that the SSL RF resonator has better matching condition compared with the general RF resonator.

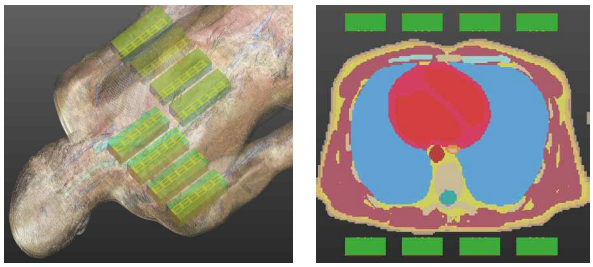

Figure 5. 8-channel body coil with human model (a) and a realistic body model including many different tissue types on axial view.

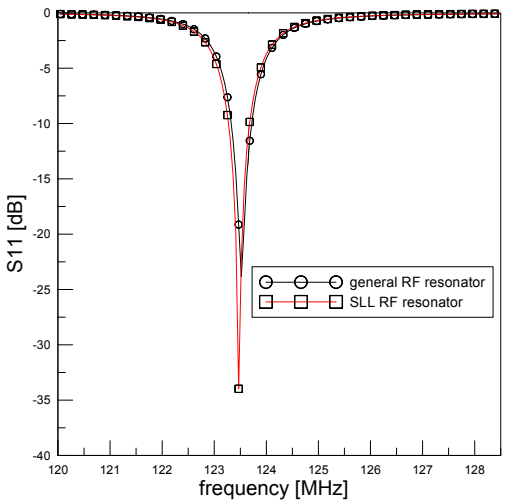

Figure 6. Frequency response of RF resonators.

Fig. 7 shows the B_1^+ field distribution of 8-channel volume coil using the general RF resonator with no optimization and with optimization on axial view. The B_1^+ field is calculated to control effectively the magnitude and phase of each RF resonator for optimization. To determine the input excitation values of each resonator element, convex optimization is used for the B_1^+ shimming [7]. When The B_1^+ field was calculated with parallel excitations, the input power of RF resonators is also normalized to the same input power (1 Watt). The total peak B_1^+ value with no optimization and optimization is 0.036 (T) and 0.041 (T), respectively. The B_1^+ field distribution of the 8-channel volume coil using the SSL RF resonator with no optimization and optimization is shown in Fig. 8. The total peak B_1^+ with no optimization and optimization is 0.036 (T) and 0.042 (T), respectively. Compared to the total B_1^+ value after optimization, the general RF resonator and SSL RF resonator are 12.6 % and 17.4 % larger than those before optimization. Table I shows the B_1^+ total, mean, and standard value of each 8-channel body coil. In the optimization results, the B_1^+ total value of the 8-channel body coil using SSL RF resonators is 3.29 % larger than it is using general RF resonator. The 8-channel body coil with

SSL RF resonators at the average value is also 3.27 % increased.

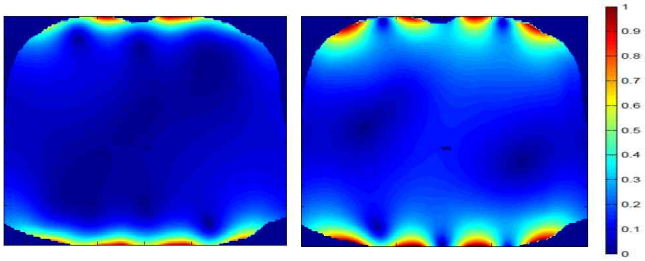

(a) (b)

Fig. 7. B_1^+ field distribution of 8-channel volume coil using the general RF resonator with no optimization (a) and optimization (b)

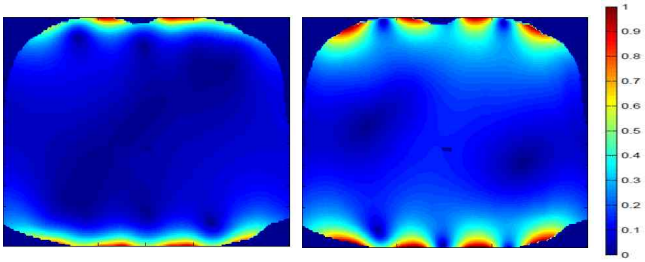

(a) (b)

Fig. 8. B_1^+ field distribution of 8-channel volume coil using SSL RF resonator with no optimization (a) and optimization (b) on axial view.

TABLE I
COMPARISON OF THE B_1^+ TOTAL, AVERAGE, AND STANDARD VALUE BETWEEN BODY COILS

	No optimization			Optimization		
Body coil	Sum (T)	Mean (μT)	Std. (μT)	Sum (T)	Mean (μT)	Std. (μT)
General RF resonator	0.036	0.5589	0.7144	0.0410	0.629	0.5267
SSL RF resonator	0.036	0.5538	0.6971	0.0423	0.650	0.5368

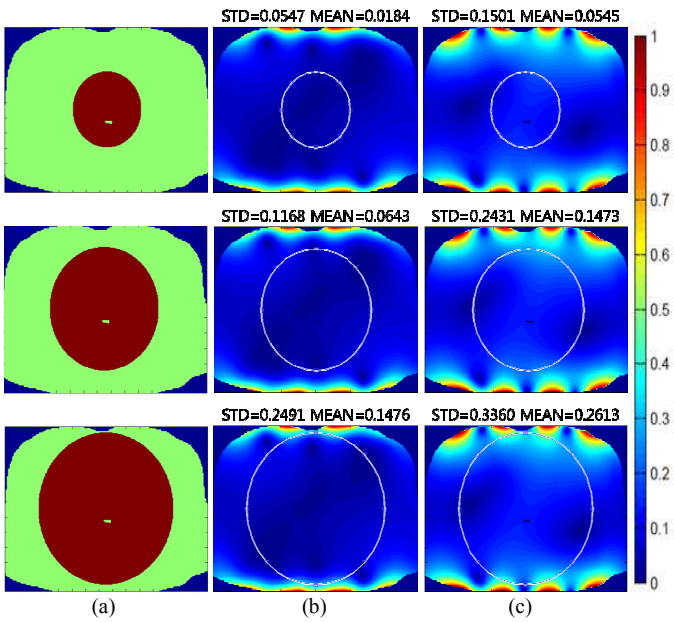

(a) (b) (c)

Fig. 9. The B_1^+ standard and mean value of the 8-channel body coil using general RF resonator are obtained for three different region of interest(ROI) (a) with no optimization (b) and optimization (c).

Fig. 9 and Fig. 10 illustrate that the B_1^+ standard and mean value of the 8-channel body coil using general RF resonator and SSL RF resonator are obtained for three different region of interest (ROI) under no optimization and optimization. The ROIs size are circles with radius 5 cm, 8 cm, and 10 cm at the center of transaxial slice, respectively. In case of three different ROI (5 cm, 8 cm, and 10 cm), the B_1^+ mean value of that is 4 % larger approximately than the 8-channel body coil using general RF resonator. As the results, the B_1^+ field of the 8-channel body coil using SSL RF resonators penetrated deep into human body and homogenized compared with the 8-channel body coil using general RF resonators.

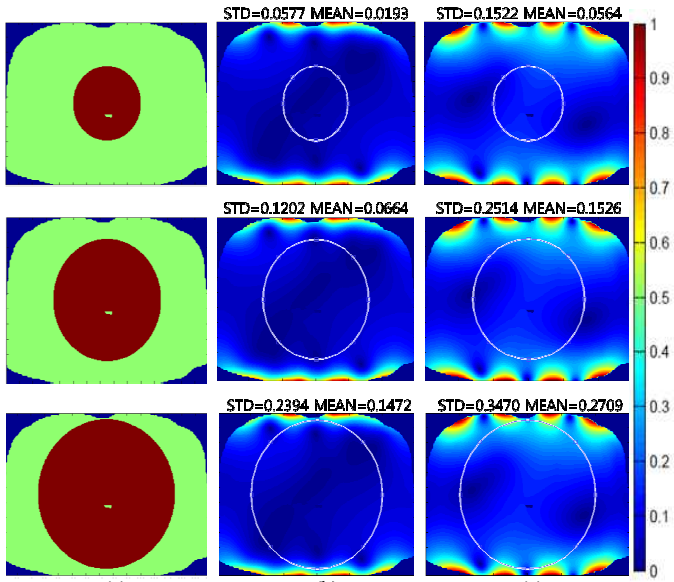

(a) (b) (c)

Fig. 10. The B_1^+ standard and mean value of the 8-channel body coil using SSL RF resonator are obtained for three different region of interest (ROI) (a) with no optimization (b) and optimization (c).

IV. CONCLUSION

3 T MRI systems have become a standard technique for diagnosis imaging of the human body. However, compared to ultra-high field MRIs (> 7 T), 3 T MRI have a worse intrinsic SNR. To overcome this problem, we propose a multichannel coil with eight SSL RF resonators and compared to traditional RF resonator based coils. From numerical simulations based on FDTD method, it was estimated that the RF magnetic field of the SSL RF resonator is stronger than the general RF resonator. After optimization, the B_1^+ total and average value are 4 % larger. As the result, the volume coil using SSL RF resonator is controlled effectively to parallel excitations for increasing the B_1^+ field and mitigating the inhomogeneous B_1^+ field at 3 T.

REFERENCES

[1] J. Vaughan, M. Garwood, C.M. Collins, W. Liu, L. DelaBarre, G. Adriany, P. Andersen, H. Merkle, R. Goebel, M.B. Smith, and K. Uğurbil, "7T vs. 4T: RF power, homogeneity, and signal-to-noise comparison in head images," *Magn Reson Med*, vol. 46, no. 1, pp. 24-30, 2001.

[2] J. Vaughan, L. DelaBarre, C. Snyder, J. Tian, C. Akgun, D. Shrivastava, W. Liu, C. Olson, G. Adriany, J. Strupp, P. Anderson, A. Gopinath and P. Moortele, Magn. Reson. Med.56,1274(2006)

[3] J. Vaughan, G. Adriany, C. J. Snyder, J. Tian, T. Thiel, L. Bolinger, H. Liu, L. DelaBarre and K. Ugurbil, Magn. Reson. Med. 52, 851(2004)

[4] X. Zhang, K. Ugurbil and W. Chen, Magn. Reson. Med. 46, 443(2001)

[5] G. Adriany, P-F. V. Moortele, F. Wiesinger, S. Moeller, J. P. Strupp, P. Anderson, C. Snyder, X. Zhang, W. Chen, K. P. Pruessmann, P. Boesiger, T. Vaughan and K. Ugurbil, Magn. Reson. Med. 53, 434(2005)

[6] SEMCAD X by SPEAG, www.speag.com

[7] H. Yoo, A. Gopinath and J. T. Vaughan, IEEE Trans. Biomed. Eng. 59(12), 3365(2012)